ENVIRONMENTAL RESEARCH
LETTERS

LETTER • **OPEN ACCESS**

Climate drivers of global wildfire burned area

To cite this article: Manolis Grillakis *et al* 2022 *Environ. Res. Lett.* **17** 045021

View the article online for updates and enhancements.

You may also like

- Anthropogenic climate change contribution to wildfire-prone weather conditions in the Cerrado and Arc of deforestation
Sihan Li, Sarah N Sparrow, Friederike E L Otto et al.

- Climate change is increasing the likelihood of extreme autumn wildfire conditions across California
Michael Goss, Daniel L Swain, John T Abatzoglou et al.

- Enhancing the fire weather index with atmospheric instability information
Miguel M Pinto, Carlos C DaCamara, Alexandra Hurduc et al.

This content was downloaded from IP address 155.198.10.231 on 08/06/2022 at 16:48

ENVIRONMENTAL RESEARCH
LETTERS

LETTER

Climate drivers of global wildfire burned area

Manolis Grillakis[1,2,*], **Apostolos Voulgarakis**[1,2,3], **Anastasios Rovithakis**[1,2], **Konstantinos D Seiradakis**[1,2], **Aristeidis Koutroulis**[1], **Robert D Field**[4,5], **Matthew Kasoar**[2,3], **Athanasios Papadopoulos**[1] and **Mihalis Lazaridis**[1]

[1] School of Chemical and Environmental Engineering, Technical University of Crete, Chania, Greece
[2] Leverhulme Centre for Wildfires, Environment and Society, Imperial College London, London, United Kingdom
[3] Department of Physics, Imperial College London, London, United Kingdom
[4] Department of Applied Physics and Applied Mathematics, Columbia University, New York, NY, United States of America
[5] NASA Goddard Institute for Space Studies, New York, NY, United States of America
[*] Author to whom any correspondence should be addressed.

E-mail: grillakis@hydrogaia.gr

Keywords: fire weather index, burned area, climate sensitivity

Supplementary material for this article is available online

OPEN ACCESS

RECEIVED
30 December 2021

REVISED
14 March 2022

ACCEPTED FOR PUBLICATION
21 March 2022

PUBLISHED
1 April 2022

Original content from this work may be used under the terms of the Creative Commons Attribution 4.0 licence.

Any further distribution of this work must maintain attribution to the author(s) and the title of the work, journal citation and DOI.

Abstract

Wildfire is an integral part of the Earth system, but at the same time it can pose serious threats to human society and to certain types of terrestrial ecosystems. Meteorological conditions are a key driver of wildfire activity and extent, which led to the emergence of the use of fire danger indices that depend solely on weather conditions. The Canadian Fire Weather Index (FWI) is a widely used fire danger index of this kind. Here, we evaluate how well the FWI, its components, and the climate variables from which it is derived, correlate with observation-based burned area (BA) for a variety of world regions. We use a novel technique, according to which monthly BA are grouped by size for each Global Fire Emissions Database (GFED) pyrographic region. We find strong correlations of BA anomalies with the FWI anomalies, as well as with the underlying deviations from their climatologies for the four climate variables from which FWI is estimated, namely, temperature, relative humidity, precipitation, and wind. We quantify the relative sensitivity of the observed BA to each of the four climate variables, finding that this relationship strongly depends on the pyrographic region and land type. Our results indicate that the BA anomalies strongly correlate with FWI anomalies at a GFED region scale, compared to the strength of the correlation with individual climate variables. Additionally, among the individual climate variables that comprise the FWI, relative humidity and temperature are the most influential factors that affect the observed BA. Our results support the use of the composite fire danger index FWI, as well as its sub-indices, the Build-Up Index (BUI) and the Initial Spread Index (ISI), comparing to single climate variables, since they are found to correlate better with the observed forest or non-forest BA, for the most regions across the globe.

1. Introduction

Due to the existence of vegetation, atmospheric oxygen, and the widespread presence of ignition sources, wildfire has been an integral part of many of the Earth's terrestrial ecosystems [1]. Wildfires comprise a significant source of greenhouse gases and aerosols playing a key role in atmospheric radiative forcing and air quality [2–4]. In densely populated regions with extensive wildland-urban interface, wildfires usually have a direct impact in terms of fire suppression financial cost, homes and infrastructure damages, crops and livestock losses and, most importantly, human losses, injuries, long-term health implications [5] and other socioeconomic impacts [6].

Wildfire activity is controlled by weather and climate parameters either in a time window of several months by controlling biomass growth and snowpack accumulation and hence fire fuel availability, or in shorter term by determining vegetation and duff layer moisture content and, hence, their flammability

© 2022 The Author(s). Published by IOP Publishing Ltd

[7–10]. Analyzing wildfire activity at a global scale for different ecoregions, Abatzoglou *et al* [11] showed that climate variability can explain one-third of the interannual variability in burned area (BA), highlighting the controlling role of climate parameters. Further studies at a global scale have shown that temperature related indicators are the best climate predictors for BA [12, 13]. Furthermore, climate forcings on wildfire activity vary by climatic region. For example, large boreal forest fires of North America, have been correlated to weather patterns that associate with strong winds, and low precipitation conditions [14]. Ying *et al* [15], indicated that the most important climate related ignition factor for the Chinese province of Yunnan is relative humidity. For Europe, significant correlation has been detected between large wildfires and high temperature for Spain [16, 17], as well as for Italy [18], but also for Greece, along with other variables [19] such as humidity and high pressure. Further studies have shown that severe fire weather conditions associate with specific synoptic-scale atmospheric circulation patterns [20, 21]. Additional factors affecting wildfire activity and the resulting BA include land-use modification Kelley *et al* [22], as well as human fire ignitions and fire suppression media [23]. In recent decades, there has been an observed increase in the size of wildfires whose cause has been debated, with some studies attributing it to climate change [24, 25] and others to decadal climate variability [26, 27]. Furthermore, recent analyses of remotely sensed data found a decline in the total BA by as high as 25% that has been attributed to agricultural expansion and intensification in African regions previously occupied by savannas and grasslands [28, 29] and to fuel moisture antecedent and during the fire season [30]. This further entangles the relation between climate and wildfires.

Andela *et al* [31] analyzed MODIS MCD64A1 BA product for the period 2003–2016, identifying 13.3 million individual fires globally, with an average duration of 4.5 d, which varies by region and land use type. This led to the development of the Global Fire Atlas [32], an important global dataset of wildfire dynamics, among other datasets such as Copernicus Proba-V [33] and Fire CCI [34]. Despite the existence of such high resolution data, studies have mainly examined the correlation between climate variability and fire activity on longer timescales, e.g. interannual and seasonal [11, 35–37].

Several indices have been developed and are being used in order to integrate the complex interactions between climate drivers and wildfire danger [38]. Such indices include the Canadian Fire Weather Index (FWI) [39], the McArthur Forest Fire Danger Index [40] and others [41]. The FWI is probably the most extensively used fire danger estimation index Due to its simplicity and robustness, the FWI has been widely used on regional or local scales [42–44] as well as on a global scale [11, 45, 46], to estimate the resulting fire danger due to weather and climate variations. Furthermore, it has been used for fire danger forecasts as a part of European Forest Fire Information System (EFFIS) and Canadian Wildland Fire Information System (CWFIS), and also as a reanalysis product [47–49].

Given the complex influences of weather and socioeconomic factors, the quantitative assessment of the BA sensitivity to weather conditions still remains a challenge. Here, we estimate how deviations from the FWI climatology, and the anomaly in the associated weather variables, correlate to satellite observed BA changes. The analysis begins with the FWI correlation to BA, then expands to individual climate parameters and FWI sub-indices, and to the estimation of the relative BA sensitivity to different climate drivers and/or indices. For the sake of simplicity, temperature, humidity, wind, and precipitation parameters are referred to as climate variables, regardless the temporal context (i.e. weather or climate) to which they refer. This is the first study to correlate FWI and underlying climate variable anomalies to BA anomalies at a monthly basis, and to rank their relative importance at a regional scale.

2. Data and methods

2.1. The fire weather index

The FWI makes use of temperature, relative humidity, wind speed (all at local noon), as well as daily rainfall, to estimate moisture in three layers of the forest floor. This information is further processed to provide two sub-indices, the Initial Spread Index, and the Buildup index. The Initial Spread Index (ISI) is related to the short-term fuel dryness and wind speed that reflects fire's initial potential rate of spread. The Buildup Index (BUI) that reflects the long-term weather effect on the fire danger and the total amount of fuel available for combustion. The FWI combines the ISI and BUI and is an overall measure of fire danger, physically related to the fire's potential intensity.

2.2. Fire, weather and FWI data

Daily BA for years 2001–2016 from MODIS Global Land Cover Product (MCD64A1) [50] forms the basis of the analysis. This dataset provides BA globally at a resolution of 0.25° for a range of land types, from barren or sparsely vegetated regions to evergreen broadleaf forests. Along with the BA, MODIS also offers information about the quality of individual fire pixels. The quality flag meaning however may vary by region, while its interpretation should be case study specific, hence it is not considered in this work. Another limitation is that MODIS cannot discriminate between one or more actively burning hotspots within a gridcell, or to discriminate the type of thermal anomaly that creates the signal [51]. Other

known limitations of MODIS BA estimation are discussed in [52].

Following a similar definition to Abatzoglou *et al* [11], the BA of forested (i.e. the combination of evergreen and deciduous, needleleaf and broadleaf as well as mixed forests), non-forested (i.e. shrublands, savannas and grasslands) as well as their combined BA are considered. Cropland fires are excluded from the analysis as being mostly correlated to prescribed burnings [11]. Mean annual BA by type, as well as distributions by calendar month are provided in supplementary figures S1 and S2 (available online at stacks.iop.org/ERL/17/045021/mmedia).

Climate data are obtained from the Global Fire Weather Database (GFWED) [48]. The GFWED contains daily and monthly FWI data calculated from MERRA2 reanalysis [53] which is provided on a $0.625° \times 0.5°$ grid. In addition, temperature, precipitation, relative humidity, and wind speed are considered which are the four climate input values to the FWI calculations. These climate variables refer to noon values rather than daily aggregates, corresponding to the time at which daily FWI values are calculated.

2.3. Spatiotemporal aggregation

The analysis is based on linear regression between the monthly sums of BA and the respective climate variables or the indices FWI, ISI and BUI, after regridding all the data to a spatial resolution of $1° \times 1°$. The logarithm of BA is used for the analysis, as it has been found to correlate well with drought and fire indices on seasonal and interannual timescales [11, 54, 55], in a linear manner. This happens because the BA exhibits a roughly exponential change in climate driver change. Additionally, we apply a new approach to further aggregate the BA and climate and fire danger variables, which increases the correlation skill. We 'group' (or bin), the BA data by their climatological monthly mean anomaly size, rather than analyzing specific wildfire events. This aggregation by fire size anomaly, smooths out the noise added to the correlation by small-scale climate factors, topography, socioeconomic drivers, that can potentially affect BA. This analysis is performed for each one of the 14 Global Fire Emissions Database (GFED4) pyrographic macro-regions (Giglio *et al* [56]; also see figure 1). For each GFED4 region, each grid-cell and month with non-zero BA is considered as a discrete wildfire set of events, hereafter refer to as a wildfire cluster. Each cluster is the sum of several fires within the specific month and grid-cell, yet it is assumed here that these fires are probably driven by similar environmental drivers, e.g. hot weather, low moisture, and antecedent built-up drought caused by synoptic scale climatological features [20]. The normalized anomaly for each calendar month is estimated for the logarithm (base 10) of BA, as well as for the climate variables, the FWI and its sub-indices (equations (1) and (2)):

$$BAA_{m,y} = log_{10}\left(BA_{m,y}\right) - log_{10}\left(\frac{\sum BA_m}{n_m}\right), \quad (1)$$

$$XA_{m,y} = X_{m,y} - \left(\frac{\sum X_m}{n_m}\right), \quad (2)$$

where BAA is the BA anomaly, m is the calendar month and y the year, X is each climate variable, the FWI or its subindices, n is their count, while the XA is their estimated anomaly.

The clusters are grouped and averaged by the size of the estimated BA anomaly into bins. Each bin contains 400 clusters. In the cases where less nonzero clusters were available, a minimum number of 10 bins is used. This selection is based on a formal sensitivity analysis on the effect of wildfire clusters per bin (supplementary section 3). The respective procedure is performed for the climate and FWI anomalies that correspond to the above-mentioned wildfires. Finally, the Pearson's correlation coefficient is estimated for the bin averages of BA. Furthermore, since the linearity of such correlations is not proven in the literature, we also estimate the Spearman's rank coefficient estimated for comparison purposes. The procedure is repeated for each GFED region and for the forest and non-forest BA types, as well as their combination. A step-by-step guide of the procedure is provided in supplementary figure S3.

To estimate the potentially most influential parameters affecting each type of BA, the slope of the regression between the BA and the different climate parameters and indices is assessed. To ensure comparability among the BA sensitivity to the different variables, a mean–standard deviation normalization (supplementary material equation (1)) is performed before the estimation and comparison of the regression slopes. To apply this type of normalization, the normality of the anomalies is tested using a Kolmogorov—Smirnov (KS) test, which shows that in the vast majority of the variables, their anomalies are normally distributed (supplementary table S3).

3. Results

3.1. Spatial patterns of BA-FWI correlation

Monthly aggregates of BA anomalies are correlated to FWI anomalies at a grid-cell scale (figure 1), for forest land type BA, non-forest, and their combined total BA. Grid-cells with less than 5 months of observed BA are omitted, to avoid artificially high Pearson's r. Results reveal several regions with high correlation coefficient (Pearson's r), in the range of 0.6–0.9. These regions are primarily located in the tropical and subtropical regions within Southern Hemisphere

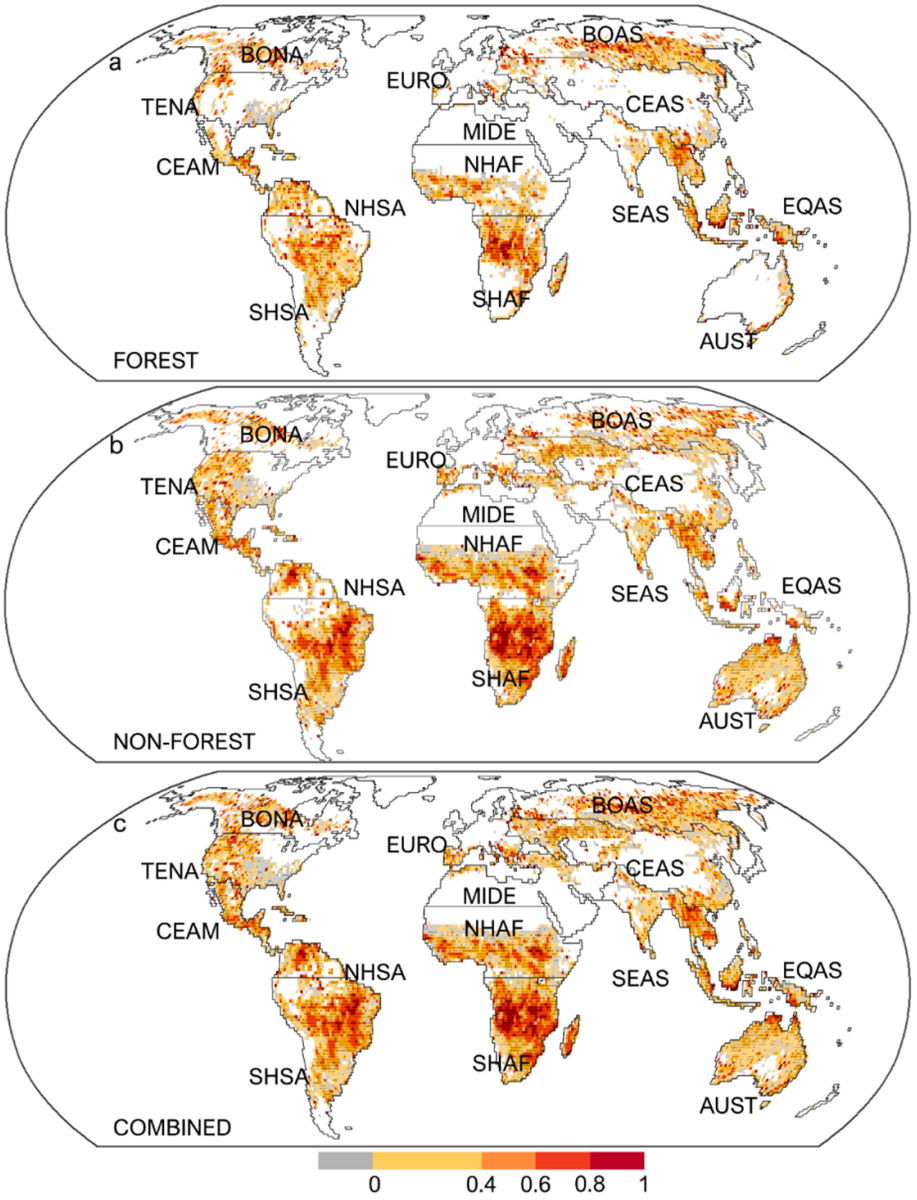

Figure 1. Pearson's correlation between monthly FWI and total burned area (log10) anomalies, for the period 2001–2016, for (a) forest land type, (b) non-forest land type, and (c) their combined burned area. Stippled regions define significant correlation at a 95% confidence level. Grid-cells with less than 5 months of observed burned area are omitted. Regional means are provided in supplementary table S1. BONA: boreal North America; TENA: temperate North America; CEAM: central America; NHSA: Northern Hemisphere South America; SHSA: Southern Hemisphere South America; EURO: Europe; MIDE: Middle East; NHAF: Northern Hemisphere Africa; SHAF: Southern Hemisphere Africa; BOAS: boreal Asia; CEAS: central Asia; SEAS: Southeast Asia; EQAS: equatorial Asia; AUST: Australia.

South America and Southern Hemisphere Africa, but also within equatorial Asia and Northern Hemisphere Africa also to a lesser extent. Interestingly, the tropical rainforest regions of the Amazon and Congo basins, as defined by Koppen-Geiger's Af scale [57] do not exhibit good correlation. Parts of the boreal forest regions also exhibit moderate to high correlation skill. For the total BA correlation to FWI (figure 1(c)), a rough 42% of the grid-cells that exhibit any correlation, show statistical significance at 95% level. The region with the highest rate of significant positive correlation is Southern Hemisphere Africa (82%), followed by central America, Northern and Southern Hemisphere South America, and equatorial Asia each to approximately 60% of grid-cells. Comparing the respective analysis between the forest and non-forest BA land types (figures 1(a) and (b)), the latter exhibits a slightly higher correlation skill (supplementary figure S4). Overall, the correlation of ungrouped values at the gridpoint scale is shown to exhibit moderate skill. The highest regional average Pearson's r is the one of Southern Hemisphere Africa for non-forest BA, with most of the regions and BA land types being significantly lower (supplementary table S1).

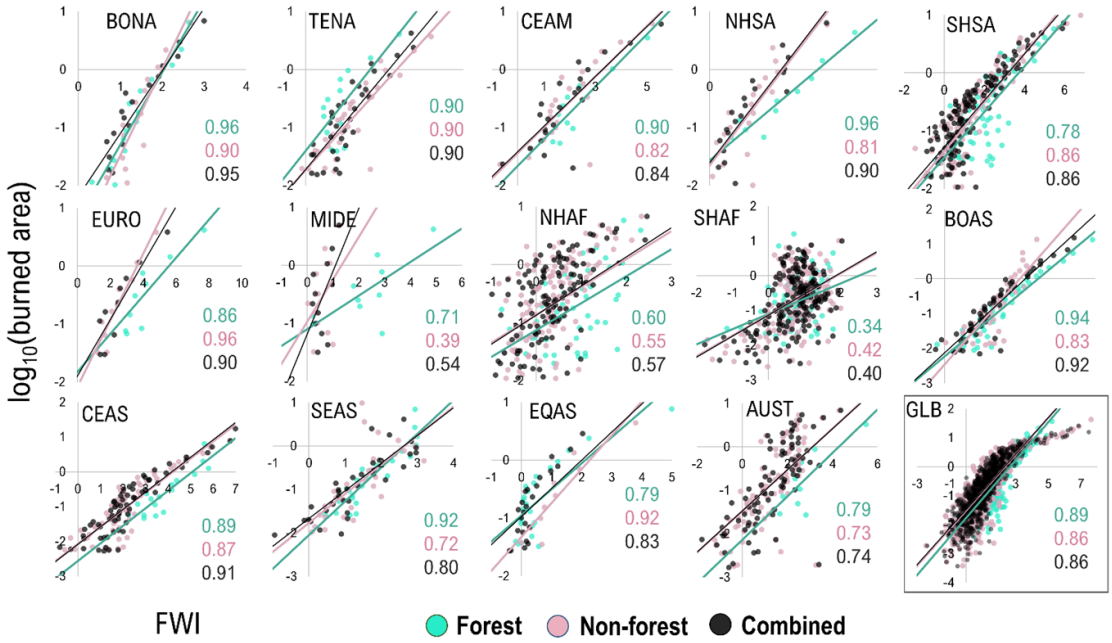

Figure 2. Correlation between FWI anomaly and log10(burned area) anomaly per region. Each scatterplot and burn area type consist of a number of points indicated in the supplementary figure S9. Pearson's correlations of forest, non-forest and total burned area are shown. The region definitions are depicted on the map of figure 1. Subplots axes scales were optimized individually.

3.2. Bin based correlation analysis

When the binning procedure is applied to the 14 GFED regions, the attained correlations become stronger. Figure 2 shows the Pearson's correlations between monthly BA anomaly and the respective FWI anomaly. Correlations are found to vary with the BA land type and region, however, in most of the regions, the correlations have a Pearson's $r > 0.7$. Exceptions to this are the Middle East, where the non-forest Pearson's r is very low, as well as for the Northern and Southern Hemisphere Africa regions. The FWI values in figure 2 are highly positive, even though they refer to anomalies, since wildfires are mostly occurring on periods with positive FWI anomalies. It is worth noting that for boreal North America and temperate North America for which the FWI was designed, the FWI correlates best with forest BA. This is also the case for the boreal Asia regions which has a comparable land cover to boreal North America. We also note that the Pearson's correlation between total BA and FWI anomalies is overall closer to the respective non-forest correlation, since the number of the cell-months with a non-zero non-forest BA is larger than for forest BA, (supplementary figure S5). It is worth noting that Spearman's rank correlation coefficient results are similar to those of Pearson's r (supplementary figure S6).

We next extend the correlation analysis to study the influence of individual climate variables involved in the FWI calculation, as well as the FWI sub-indices, ISI and BUI. We find that the FWI or ISI and BUI subindices typically exhibit stronger correlations to BA than individual climate variables (figure 3). This indicates that more synthetic variables can be better predictors of BA for the majority of regions. Only for a few GFED regions and land types may a climate variable marginally surpass in correlation skill the FWI or its subindices. This is the case for forest BA in temperate North America, Middle East, equatorial Asia, and Australia, as well as boreal Asia for the case of non-forest BA. It is worth noting that even on a global scale, this type of analysis reveals a good correlation skill (>0.7 in the case of synthetic indices).

3.3. Burned area sensitivity assessment

In figure 4, the four climate variables are sorted by their descending normalized sensitivity. Hence, this shows which individual climate variable anomaly is more associated with the BA anomaly, suggesting which variables may be the key drivers of the BA anomaly. The ISI and BUI are also sorted accordingly. In the case of forest BA anomaly, it is shown that it is most sensitive to relative humidity anomalies for 11 out of 14 regions. For the non-forest BA anomaly, 10 out of 14 regions are most sensitive to the respective relative humidity or temperature anomaly. The combined BA anomaly in 13 out of 14 regions is mostly sensitive to temperature or relative humidity anomaly. Further, for both forest and non-forest BA anomaly, the regions most sensitive to BUI or ISI are almost equally split, but do not coincide. Finally, for the combined BA anomaly, results resemble those found for the non-forest regions' BA.

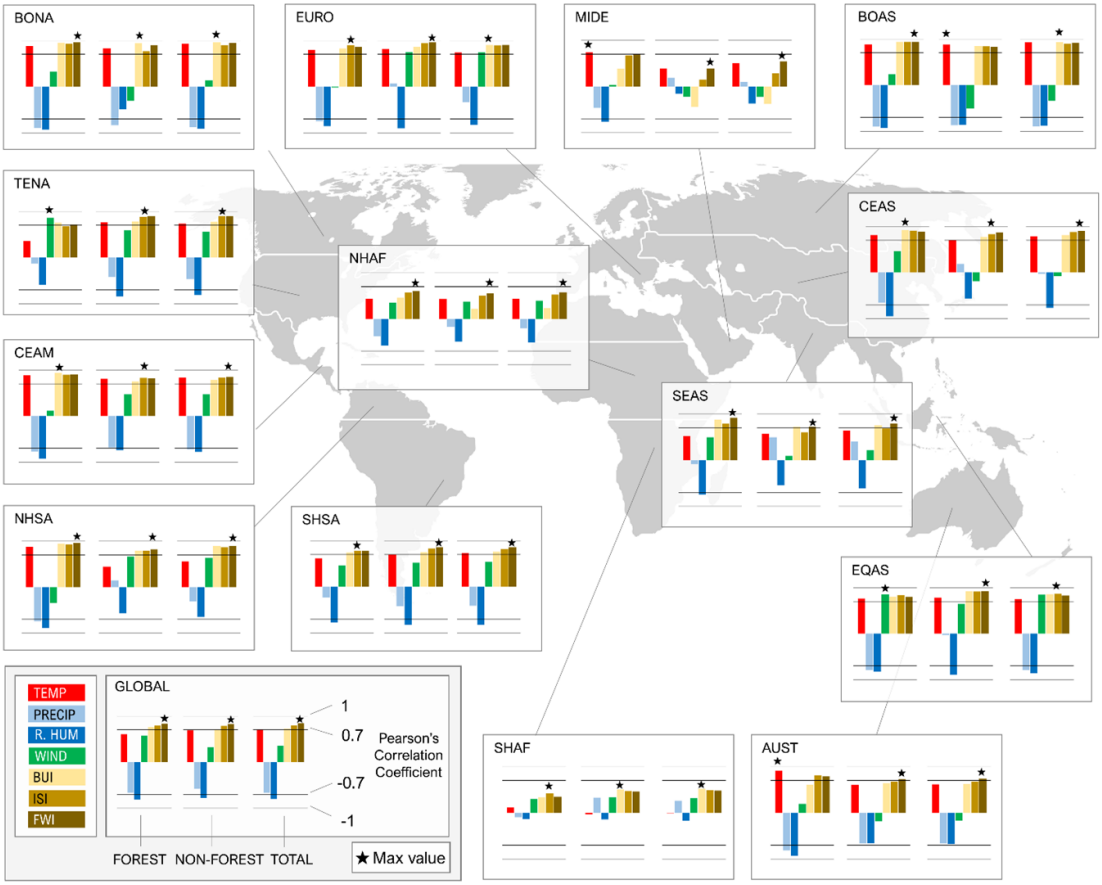

Figure 3. Pearson's correlation of anomalies in each climate parameter, the FWI and its subindices, with the BA anomalies. In each bar plot, the correlation for temperature (TEMP), precipitation (PRECIP), relative humidity (R. HUM), wind, initial spread index (ISI), buildup index (BUI) and fire weather index (FWI) are shown, respectively. The three bar charts per region show the correlations for the forest BA, non-forest BA and total BA. Brown columns of FWI correlation are the same as in figure 2. Stars indicate the best correlating parameter. Numerical values of the correlations are provided in supplementary table S2.

4. Discussion

We show that individual climate parameters as well as their corresponding FWI and subindices, correlate well to BA of both forest and non-forest areas, as well as their combination. The grid-cell level analysis (figure 1) is in broad agreement with the ecoregion-based analysis of Abatzoglou *et al* [11]. Differences between the FWI and forest and non-forest BA, over the regions boreal North America, temperate North America and boreal Asia, agree with those in Abatzoglou *et al* [11], for their North America and Russia regions. Moreover, at lower latitudes, there is general agreement in correlation over Central and South America, the forested regions of equatorial Asia, and southeastern Australia. The greatest differences to our results are found over Africa, for which our regions of coherent positive correlations appear to be weaker in their study for forest BA and largely absent for non-forest BA.

The regression analysis with binned data according to BA magnitude, shows that there is a clear meteorological forcing of the anomaly of BA at a monthly timescale, which is found to become even stronger correlating to the FWI. Further, it shows that the FWI correlation to the BA using the binning method is generally higher than the grid-cell level correlation. Exceptions are the Northern but most importantly Southern Hemisphere Africa, the SHAF which is a hotspot of global wildfire activity. This may be explained by the results of Chuvieco *et al* [58], who show that Northern and Southern Hemisphere Africa are the two region in which the BA annual variability is strongly controlled by socio-economic factors, as captured by the human development index (HDI) and Gross Domestic Production per capita (GDP). Similar results about the BA and FWI anomalies correlation are reported by Tian *et al* [59] for China.

Globally, in the case of forest BA anomaly, the most highly associated climate variable is found to be relative humidity, while in the case of the non-forest BA anomaly, temperature and relative humidity are found to be most highly associated for most of the regions, without, however, exhibiting any clear spatial or latitudinal pattern. The most highly associated variables for the combined BA anomaly are similar to those for the non-forest BA. Similarly, Krawchuk *et al* [60], mention that net primary productivity,

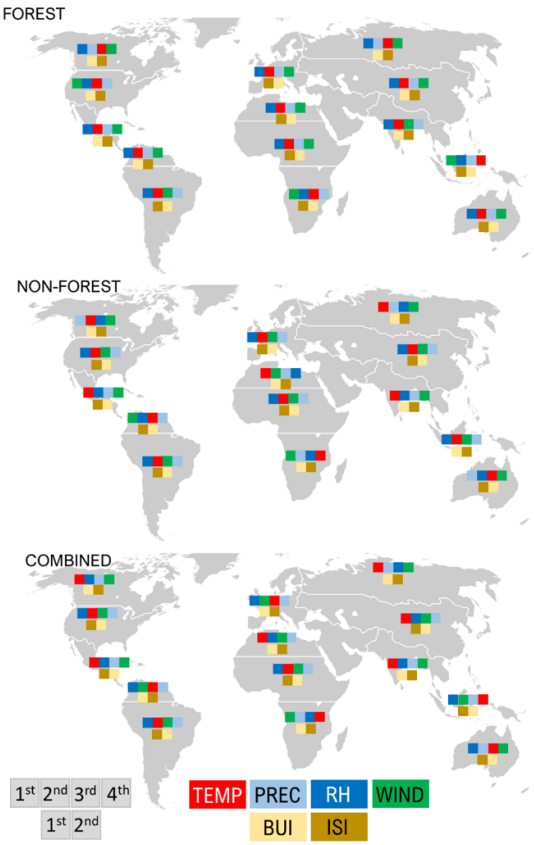

Figure 4. The sequence of the upper four squares indicates the most to least affecting climate variable for each region's BA. The sequence of the two lower squares indicates the most and less affecting parameter between BUI and ISI. Normalized slopes are provided in supplementary table S4.

mean temperature of the warmest month and precipitation are the three most important variables affecting fire probability at a global scale. Further regional comparisons reveal patterns of similarities and differences. Most notable similarities are those of forest BA, where the boreal regions (boreal North America, boreal Asia) show increased sensitivity to dry (low RH) and arid (low precipitation) conditions, while temperature along with wind are ranked last. Sedano and Randerson [61], analyzed wildfire data for Alaska during 2002–2011, finding a significant correlation between daily VPD and likelihood that a lightning strike would develop into a fire ignition, in line with our results for the boreal North America. Regarding temperate North America, Mueller *et al* [62] studied climate and wildfire relationships for Arizona and New Mexico, indicating strong relationships between the annual BA and wildfire severity with vapor pressure deficit (VPD) which links to low atmospheric humidity. In the same line are the results of Li and Banerjee [63], who found that regions in California with high temperature and high VPD exhibit high risk of wildfire occurrence. Furthermore, Ying *et al* [15] tested a range of climate and socioeconomic wildfire ignition factors for China, indicating that the most important climate factor is low relative humidity, in line with our results for central Asia.

When it comes to the sub-indices, BUI is consistently more important than the ISI sub-index in boreal regions, suggesting a greater role of season-scale drying. The relative humidity and temperature variables are the most commonly influential parameters elsewhere across the globe (central America, northern and southern Hemisphere South America, Europe, Middle East, Northern Hemisphere Africa, central Asia, southeast Asia, Australia), usually followed by precipitation, except for the cases of Southern Hemisphere South America and Southeast Asia, where wind is the third most influential variable. This similarity may be attributed to the monsoonal circulation patterns that affect both regions [64]. Furthermore, Southern Hemisphere Africa and equatorial Asia BA are found to be mostly affected positively by wind and negatively by precipitation, which is probably related to the strong effect of ENSO periodic variation that causes synchronized warm and dry conditions, and enhanced eastern winds over eastern Africa [65]. Furthermore, those regions' forest BA is most sensitive to ISI. For the non-forest regions, BA is mostly sensitive to temperature and relative humidity (temperate North America, central America, Southern Hemisphere South America, Europe, Northern Hemisphere Africa, central Asia, Southeast Asia, Australia), generally followed by wind rather than precipitation, with exceptions to the latter being the cases of central Asia and Southeast Asia. Similarities are also found for the boreal (boreal North America, boreal Asia) regions, where precipitation and temperature are the two most influential variables in all those regions. A notable difference comparing the forest and non-forest most influential climate variables for BA is that in the latter there are more regions in which temperature is the first or second most influential variable (boreal North America, boreal Asia, temperate North America, equatorial Asia). This is to some extent intuitive, since forests are more resilient to heatwaves and hence to the consequent associated wildfires, compared to non-forest areas [66]. In contrast to those four regions, Australia exhibits the opposite behavior, with temperature being one of the top two most influential variables for the forest BA but not for the non-forest BA.

This work focused solely in analyzing the BA and did not expand to other important wildfire aspects. Fire severity for example [67] has been found to be an equally important fire behaviour property. Additionally, we assume that the reanalysis climate variables adequately represent the past climate conditions for the period of months determining the FWI preceding the wildfires. Another caveat of the analysis stems from the limitations of MCD64A1 BA product that has a minimum detectable burn size of 40 ha, and also may underestimate the BA in specific regions due to cloudiness [52]. An assumption that needs to be

discussed is the one made about the stationarity in the climate-wildfire interlinkages for the study period. This is particularly important for both BA and the climate variables. For example, Zhuang *et al* [68] highlight the role of VPD in wildfire for the Western US, detecting a positive trend in VPD between 1979–2000 which was attributed to anthropogenic warming. In the same line, Abram *et al* [69] show a positive VPD trend in the last decade for Australia. Such changes within the study period challenge the normalization that is performed in the studied variables. Accordingly, as discussed earlier, the BA has been detected to decline in Northern and Southern Hemisphere Africa as a result of agricultural expansion and intensification in regions previously occupied by savannas and grasslands [28, 29, 70]. This may also explain the poor correlations obtained for Northern and southern Hemisphere Africa regions in the current study. Finally, it has to be stressed that the presented regression analyses between specific climate variables and BA, cannot be used as a prediction tool, since the climatic parameters and indices were analyzed independently, disregarding the synergy between them, and because the analysis is performed by preselecting gridcell-months with already recorded BA.

5. Conclusions

This work focuses on exploring the correlation and determining the relative sensitivity of BA to major climatic drivers, as well as the FWI and its sub-indices, by adopting a novel correlation approach based on the binning of data based on the BA size. This type of analysis is shown to be powerful as it reveals significant correlations on both regional and global scales, for forest and non-forest BA, as well as their combination. The region-specific sensitivity of BA to each climatological parameter may serve as a benchmarking tool for fire-enabled vegetation models and intercomparison projects such as FireMIP [13, 71] and ISIMIP [72]. This type of analysis can also facilitate the attribution of specific wildfire events to the variability of specific climate parameters by comparing the specific event's climatic conditions to the climatic conditions of other BA events of the same class. Since this is the first study that ranks the relative effect of the four analyzed climate variables to the observed BA, the results of this work support the better understanding of the climatic control on wildfires and hence aim towards a more proactive wildfire management.

Data availability statement

The climate and FWI data used in this study were obtained from the NASA Center for Climate Simulation, available at: https://portal.nccs.nasa.gov/datashare/GlobalFWI/v2.0/fwiCalcs.MERRA2/Default/MERRA2/; https://portal.nccs.nasa.gov/datashare/GlobalFWI/v2.0/wxInput/MERRA2/ The data that support the findings of this study are available upon reasonable request from the authors.

Acknowledgments

This work was funded by the CLIMPACT—National Research Network on Climate Change and its Impacts project, financed by the Public Investment Program of Greece and supervised by General Secretariat for Research and Technology (GSRT). Also, this research was partially funded by the Leverhulme Centre for Wildfires, Environment, and Society through the Leverhulme Trust, Grant No. RC-2018-023.

We acknowledge the NASA and MODIS for providing the MCD64A1 burned area product, as well as NASA's Global Fire WEather Database (GFWED) from which the FWI and the climate parameters were obtained.

ORCID iDs

Manolis Grillakis https://orcid.org/0000-0002-4228-1803
Anastasios Rovithakis https://orcid.org/0000-0001-6072-5298
Aristeidis Koutroulis https://orcid.org/0000-0002-2999-7575

References

[1] Bowman D M J S *et al* 2009 Fire in the earth system *Science* **324** 481–4
[2] Urbanski S 2014 Wildland fire emissions, carbon, and climate: emission factors *For. Ecol. Manage.* **317** 51–60 Available from
[3] Voulgarakis A and Field R D 2015 Fire influences on atmospheric composition, air quality and climate *Curr. Pollut. Rep.* **12** 70–81
[4] Lasslop G *et al* 2019 Influence of fire on the carbon cycle and climate *Curr. Clim. Change Rep.* **52** 112–23
[5] Kochi I *et al* 2010 The economic cost of adverse health effects from wildfire-smoke exposure: a review *Int. J. Wildland Fire* **19** 803
[6] Rosenthal A, Stover E and Haar R J 2021 Health and social impacts of California wildfires and the deficiencies in current recovery resources: an exploratory qualitative study of systems-level issues *PLoS One* **16** e0248617
[7] Kitzberger T *et al* 2017 Direct and indirect climate controls predict heterogeneous early-mid 21st century wildfire burned area across western and boreal North America *PLoS One* **12** e0188486
[8] Hou X and Orth R O S 2020 Observational evidence of wildfire-promoting soil moisture anomalies *Sci. Rep.* **10** 1–8
[9] Gudmundsson L *et al* 2014 Predicting above normal wildfire activity in southern Europe as a function of meteorological drought *Environ. Res. Lett.* **9** 084008
[10] Kuhn-Régnier A *et al* 2021 The importance of antecedent vegetation and drought conditions as global drivers of burnt area *Biogeosciences* **18** 3861–79
[11] Abatzoglou J T *et al* 2018 Global patterns of interannual climate–fire relationships *Glob. Change Biol.* **24** 5164–75
[12] Bistinas I *et al* 2014 Causal relationships versus emergent patterns in the global controls of fire frequency *Biogeosciences* **11** 5087–101

[13] Forkel M et al 2019 Emergent relationships with respect to burned area in global satellite observations and fire-enabled vegetation models Biogeosciences 16 57–76
[14] Macias Fauria M and Johnson E A 2008 Climate and wildfires in the North American boreal forest Phil. Trans. R. Soc. B 363 2317–29
[15] Ying L et al 2021 Relative humidity and agricultural activities dominate wildfire ignitions in Yunnan, Southwest China: patterns, thresholds, and implications Agric. For. Meteorol. 307 108540
[16] Molina-Terrén D M and Cardil A 2016 Temperature determining larger wildland fires in NE Spain Theor. Appl. Climatol. 125 295–302
[17] Cardil A, Eastaugh C S and Molina D M 2015 Extreme temperature conditions and wildland fires in Spain Theor. Appl. Climatol. 122 219–28
[18] Cardil A et al 2014 Large wildland fires and extreme temperatures in sardinia (Italy) iFor.- Biogeosci. For. 7 162
[19] Papadopoulos A et al 2013 Investigating the relationship of meteorological/climatological conditions and wildfires in Greece Theor. Appl. Climatol. 112 113–26
[20] Crimmins M A 2006 Synoptic climatology of extreme fire-weather conditions across the southwest United States Int. J. Climatol. A 26 1001–16
[21] Williams A P et al 2014 Causes and implications of extreme atmospheric moisture demand during the record-breaking 2011 wildfire season in the southwestern United States J. Appl. Meteorol. Climatol. 53 2671–84
[22] Kelley D I et al 2019 How contemporary bioclimatic and human controls change global fire regimes Nat. Clim. Change 9 690–6
[23] Oliveira S and Zêzere J L 2020 Assessing the biophysical and social drivers of burned area distribution at the local scale J. Environ. Manage. 264 110449
[24] Reilly M J et al 2017 Contemporary patterns of fire extent and severity in forests of the Pacific Northwest, USA (1985–2010) Ecosphere 8 e01695
[25] Singleton M P et al 2019 Increasing trends in high-severity fire in the southwestern USA from 1984 to 2015 For. Ecol. Manage. 433 709–19
[26] Hanson C T and Odion D C 2016 Historical forest conditions within the range of the Pacific fisher and spotted owl in the central and Southern sierra Nevada, California, USA Nat. Areas J. 36 8–19
[27] Baker W L 2015 Historical Northern spotted owl habitat and old-growth dry forests maintained by mixed-severity wildfires Landsc. Ecol. 30 655–66
[28] Andela N et al 2017 A human-driven decline in global burned area Science 356 1356–62
[29] Jiang Y, Zhou L and Raghavendra A 2020 Observed changes in fire patterns and possible drivers over Central Africa Environ. Res. Lett. 15 940–8
[30] Zubkova M et al 2019 Changes in fire activity in Africa from 2002 to 2016 and their potential drivers Geophys. Res. Lett. 46 7643–53
[31] Andela N et al 2019 The global fire atlas of individual fire size, duration, speed and direction Earth Syst. Sci. Data 11 529–52
[32] Andela N 2019 Fire atlas—global fire emissions database (Accessed 23 December 2021) (available at: www.globalfiredata.org/fireatlas.html)
[33] Tansey K et al 2008 A new, global, multi-annual (2000–2007) burnt area product at 1 km resolution Geophys. Res. Lett. 35 1–6
[34] Chuvieco E et al 2016 A new global burned area product for climate assessment of fire impacts Glob. Ecol. Biogeogr. 25 619–29
[35] Harris S et al 2020 The sensitivity of fire activity to interannual climate variability in victoria, Australia J. South Hemisph. Earth Syst. Sci. 69 146–60
[36] Bedia J et al 2015 Global patterns in the sensitivity of burned area to fire-weather: implications for climate change Agric. For. Meteorol. 214–215 369–79
[37] Chen Y et al 2016 How much global burned area can be forecast on seasonal time scales using sea surface temperatures? Environ. Res. Lett. 11 045001
[38] de Groot W J, Wotton B M and Flannigan M D 2015 Wildland fire danger rating and early warning systems Wildfire Hazards, Risks and Disasters (Amsterdam: Elsevier) ed Paton D pp 207–28 ch 11
[39] Van Wagner C E 1974 Structure of the Canadian forest fire weather index
[40] Noble I R, Gill A M and Bary G A V 1980 McArthur's fire-danger meters expressed as equations Aust. J. Ecol. 5 201–3
[41] Matthews S 2009 A comparison of fire danger rating systems for use in forests Aust. Meteorol. Oceanogr. J. 58 41
[42] Viegas D X et al 2000 Comparative study of various methods of fire danger evaluation in Southern Europe Int. J. Wildland Fire 9 235–46
[43] Dimitrakopoulos A P, Bemmerzouk A M and Mitsopoulos I D 2011 Evaluation of the Canadian Fire Weather Index system in an eastern Mediterranean environment Meteorol. Appl. 18 83–93
[44] Cruz M G et al 2012 Anatomy of a catastrophic wildfire: the Black Saturday Kilmore East fire in Victoria, Australia For. Ecol. Manage. 284 269–85
[45] Jolly W M et al 2015 Climate-induced variations in global wildfire danger from 1979 to 2013 Nat. Commun. 6 1–11
[46] Abatzoglou J T, Williams A P and Barbero R 2019 Global emergence of anthropogenic climate change in fire weather indices Geophys. Res. Lett. 46 326–36
[47] Vitolo C et al 2019 Data descriptor: a 1980–2018 global fire danger re-analysis dataset for the Canadian fire weather indices Sci. Data 6 1–10
[48] Field R D 2020 Evaluation of global fire weather database reanalysis and short-term forecast products Nat. Hazards Earth Syst. Sci. 20 1123–47
[49] Field R D et al 2015 Development of a global fire weather database Nat. Hazards Earth Syst. Sci. 15 1407–23
[50] Giglio L et al 2018 The collection 6 MODIS burned area mapping algorithm and product Remote Sens. Environ. 217 72–85
[51] Giglio L et al 2018 Modis collection 6 active fire product user's guide revision B (Department of Geographical Sciences University of Maryland) p 9
[52] Giglio L, Randerson J T and Van Der Werf G R 2013 Analysis of daily, monthly, and annual burned area using the fourth-generation global fire emissions database (GFED4) J. Geophys. Res. Biogeosci. 118 317–28
[53] Gelaro R et al 2017 The modern-era retrospective analysis for research and applications, version 2 (MERRA-2) J. Clim. 30 5419–54
[54] Turco M et al 2018 Exacerbated fires in Mediterranean Europe due to anthropogenic warming projected with non-stationary climate-fire models Nat. Commun. 9 1–9
[55] Zubkova M et al 2021 Conflict and climate: drivers of fire activity in Syria in the 21 st century Earth Interact. 1 1–48
[56] Giglio L et al 2006 Global estimation of burned area using MODIS active fire observations Atmos. Chem. Phys. 6 957–74
[57] Beck H E et al 2018 Present and future Köppen-Geiger climate classification maps at 1-km resolution Sci. Data 5 1–12
[58] Chuvieco E et al 2021 Human and climate drivers of global biomass burning variability Sci. Total Environ. 779 146361
[59] Tian X et al 2011 Wildfires and the Canadian forest fire weather index system for the Daxing'anling region of China Int. J. Wildland Fire 20 963–73
[60] Krawchuk M A et al 2009 Global pyrogeography: the current and future distribution of wildfire PLoS One 4 5102
[61] Sedano F and Randerson J T 2014 Multi-scale influence of vapor pressure deficit on fire ignition and spread in boreal forest ecosystems Biogeosciences 11 3739–55
[62] Mueller S E et al 2020 Climate relationships with increasing wildfire in the southwestern US from 1984 to 2015 For. Ecol. Manage. 460 117861

[63] Li S and Banerjee T 2021 Spatial and temporal pattern of wildfires in California from 2000 to 2019 *Sci. Rep.* **11** 1–17
[64] Geen R *et al* 2020 Monsoons, ITCZs, and the concept of the global monsoon *Rev. Geophys.* **58** e2020RG000700
[65] Guimarães Nobre G *et al* 2019 Achieving the reduction of disaster risk by better predicting impacts of El Niño and La Niña *Prog. Disaster Sci.* **2** 100022
[66] Van Gorsel E *et al* 2016 Carbon uptake and water use in woodlands and forests in southern Australia during an extreme heat wave event in the 'angry summer' of 2012/2013 *Biogeosciences* **13** 5947–64
[67] Hessl A E 2011 Pathways for climate change effects on fire: models, data, and uncertainties *Prog. Phys. Geogr.* **35** 393–407
[68] Zhuang Y *et al* 2021 Quantifying contributions of natural variability and anthropogenic forcings on increased fire weather risk over the western United States *Proc. Natl Acad. Sci.* **118** e2111875118
[69] Abram N J *et al* 2021 Connections of climate change and variability to large and extreme forest fires in southeast Australia *Commun. Earth Environ.* **2** 1–17
[70] Wu C *et al* 2021 Historical and future global burned area with changing climate and human demography *One Earth* **4** 517–30
[71] Rabin S S *et al* 2017 The fire modeling intercomparison project (FireMIP), phase 1: experimental and analytical protocols with detailed model descriptions *Geosci. Model Dev.* **10** 1175–97
[72] Warszawski L *et al* 2014 The inter-sectoral impact model intercomparison project (ISI–MIP): project framework *Proc. Natl Acad. Sci.* **111** 3228–32